UNC-60B, an ADF/Cofilin Family Protein, Is Required for Proper Assembly of Actin into Myofibrils in *Caenorhabditis elegans* Body Wall Muscle

Shoichiro Ono,* David L. Baillie,‡ and Guy M. Benian*

*Department of Pathology and Department of Cell Biology, Emory University, Atlanta, Georgia 30322; and ‡Institute of Molecular Biology and Biochemistry, Department of Biological Sciences, Simon Fraser University, Burnaby, British Columbia, Canada V5A 1S6

Abstract. The *Caenorhabditis elegans unc-60* gene encodes two functionally distinct isoforms of ADF/cofilin that are implicated in myofibril assembly. Here, we show that one of the gene products, UNC-60B, is specifically required for proper assembly of actin into myofibrils. We found that all homozygous viable *unc-60* mutations resided in the unc-60B coding region, indicating that UNC-60B is responsible for the Unc-60 phenotype. Wild-type UNC-60B had F-actin binding, partial actin depolymerizing, and weak F-actin severing activities in vitro. However, mutations in UNC-60B caused various alterations in these activities. Three missense mutations resulted in weaker F-actin binding and actin depolymerizing activities and complete loss of severing activity. The *r398* mutation truncated three residues from the COOH terminus and resulted in the loss of severing activity and greater actin depolymerizing activity. The *s1307* mutation in a putative actin-binding helix caused greater activity in actin-depolymerizing and severing. Using a specific antibody for UNC-60B, we found varying protein levels of UNC-60B in mutant animals, and that UNC-60B was expressed in embryonic muscles. Regardless of these various molecular phenotypes, actin was not properly assembled into embryonic myofibrils in all *unc-60* mutants to similar extents. We conclude that precise control of actin filament dynamics by UNC-60B is required for proper integration of actin into myofibrils.

Key words: myofibrils • thin filaments • ADF/cofilin • actin polymerization • *unc-60*

In striated muscles, actin and myosin are precisely aligned in a striated pattern so that they coordinately generate contractile forces. During the development of myofibrils, the assembly of these contractile proteins must be accurately regulated, but little is known about its mechanism. To control the uniform length of thin filaments, tropomodulin, which caps pointed ends of actin filaments, has been shown to be required (Gregorio et al., 1995). CapZ, a barbed end actin-capping protein is also involved in myofibril assembly (Schafer et al., 1995), which probably terminates actin assembly (Eddy et al., 1997) and regulates the length of actin filaments (Xu et al., 1999).

Another important issue in myofibrillogenesis is how the assembly of actin into myofibrils is regulated. The assembly of actin in embryonic skeletal muscle is negatively regulated. Consequently, ~40% of actin is present in a monomeric form (Shimizu and Obinata, 1986). However, as muscle develops, the concentration of monomeric actin decreases, while the total amount of actin increases by 10-fold in adult muscle (Shimizu and Obinata, 1986), indicating that myofibrillar actin is assembled from the monomer pool of both existing and newly synthesized actin molecules in developing muscle. In chicken embryonic skeletal muscle, profilin (Ohshima et al., 1989), actin depolymerizing factor (ADF[1]) (Abe and Obinata, 1989), and cofilin (Abe et al., 1989) have been identified as G-actin binding proteins that are postulated to regulate actin assembly into myofibrils. In addition, mammalian skeletal muscles express a muscle-specific isoform of cofilin (Ono et al., 1994), implicating its role during myofibril assembly. However, how the assembly of actin is initiated and how these actin binding proteins are involved in the process of actin assembly are not understood.

Address correspondence to Shoichiro Ono, Department of Pathology, Woodruff Memorial Building, Room 7125, Emory University, Atlanta, GA 30322. Tel.:(404) 727-5945. Fax: (404) 727-8540. E-mail: ono@bimcore.emory.edu

1. *Abbreviation used in this paper:* ADF, actin depolymerizing factor.

ADF (Bamburg et al., 1980) and cofilin (Nishida et al., 1984) are homologous proteins and belong to the ADF/cofilin family (Moon and Drubin, 1995). They have been shown to bind to both G- and F-actin at a stoichiometry of 1:1 and enhance turnover of actin subunits within actin filaments by severing F-actin and increasing the off rate of actin subunits from the pointed ends (Carlier et al., 1997; Du and Frieden, 1998; Maciver et al., 1991, 1998). ADF/cofilin is necessary for cytokinesis (Abe et al., 1996; Gunsalus et al., 1995), actin turnover in comet tails of *Listeria monocytogenes* (Carlier et al., 1997; Rosenblatt et al., 1997), and for in vivo actin turnover in yeast (Lappalainen et al., 1997). In addition, overexpression of cofilin in *Dictyostelium* enhances cell motility (Aizawa et al., 1996). These observations show that ADF/cofilin regulates dynamic aspects of the actin cytoskeleton in vivo. A study using systematic mutagenesis of yeast cofilin has shown that actin-depolymerizing activity of cofilin is essential for its in vivo function (Lappalainen and Drubin, 1997; Lappalainen et al., 1997). In addition, multiple isoforms of ADF/cofilin have been found in vertebrates, *C. elegans*, and maize, and show different patterns of tissue distribution (Moriyama et al., 1990; Hayakawa et al., 1993; McKim et al., 1994; Ono et al., 1994; Lopez et al., 1996). Interestingly, expression of a mammalian muscle-specific isoform (Ono et al., 1994) and maize pollen–specific isoforms (Lopez et al., 1996) are restricted in particular differentiated tissues, suggesting their specialized roles in the regulation of certain types of actin cytoskeleton.

To understand the in vivo regulation of actin assembly, we have taken genetic and biochemical approaches to analyze the *C. elegans unc-60* mutants that show abnormal assembly of actin filaments in muscle cells (Waterston et al., 1980; McKim et al., 1988). Two isoforms of ADF/cofilin, UNC-60A, and UNC-60B, are generated by alternative splicing from the *unc-60* gene (McKim et al., 1994) and have different effects on rabbit muscle actin in vitro (Ono and Benian, 1998). UNC-60A shows actin-depolymerizing activity and an inhibitory effect on actin polymerization, whereas UNC-60B binds to F-actin without significantly depolymerizing it and accelerates actin polymerization (Ono and Benian, 1998). These properties of UNC-60A and UNC-60B strongly suggest that they are functionally distinct in vivo. Here, we report that UNC-60B is required for myofibril assembly and its normal function is to regulate a dynamic state of actin filaments. Our results provide the first evidence of an isoform-specific requirement of ADF/cofilin for assembly of a differentiated actin cytoskeleton.

Materials and Methods

Nematode Strains

Wild-type *C. elegans* strain N2 was obtained from the *Caenorhabditis* Genetics stock center. *unc-60* mutants were obtained from various colleagues and their origins were described previously (McKim et al., 1988). All mutant animals used in this study were homozygous for each allele.

Motility Assay

A motility assay was performed as described by Epstein and Thomson (1974). In brief, adult nematodes carrying eggs in a single row were placed in a droplet (10 μl) of M9 buffer. One beat was counted when a worm swung its head to either right or left. The total number of beats in 1 min was recorded. The data were taken only when the worms kept beating for 1 min.

Sequencing of Genomic DNA

Genomic DNA for unc-60A (1 kb) and unc-60B (2.5 kb) were amplified from two adult worms from each strain (Barstead and Waterston, 1991) with *Pfu* DNA polymerase (Stratagene Inc.) and all of the exons were sequenced with an automated sequencer (ABI373). Sequencing was performed on at least two independent PCR products to insure that there were no PCR-induced errors. After we identified the mutation sites in *e677*, *m35*, and *r398*, we focused only on unc-60B because a fine structure map showed that the other mutations were located between *e677* and *m35* (McKim et al., 1988).

Production and Purification of Recombinant Mutant Proteins

Site-directed mutagenesis was performed on pET-UNC-60B (Ono and Benian, 1998), a bacterial expression construct for wild type (that expresses UNC-60B without any additional sequences), with a mutagenesis kit (Quick-change; Stratagene). Recombinant proteins except UNC-60B (*m35*) were expressed and purified as described previously for wild-type UNC-60B (Ono and Benian, 1998). Because a large portion of UNC-60B (*m35*) was insoluble after induction of expression, the insoluble proteins were solubilized by 6 M urea. After urea was removed by dialysis, the protein was purified with DEAE-cellulose (DE-52; Whatman), followed by gel filtration (Sephacryl S-200; Pharmacia Biotech). The concentrations of UNC-60B proteins were spectrophotometrically determined using a calculated extinction coefficient (Gill and von Hippel, 1989) of 8,040 $M^{-1}cm^{-1}$ at 280 nm.

Actin Binding Assays

Actin was purified from wild-type *C. elegans* as described previously (Ono, 1999). This actin preparation probably contains both muscle and nonmuscle actins. Nonetheless, we expect that most of this actin preparation consists of the muscle isoforms because of extensive extraction of nematodes in the early steps of the purification (for review see Ono, 1999). *C. elegans* actin was used in this study because UNC-60B interacts with *C. elegans* actin differently than rabbit muscle actin (Ono, 1999). Copelleting assays of wild-type and mutant UNC-60B proteins with *C. elegans* F-actin were performed as described previously (Ono and Benian, 1998) in a buffer containing 0.1 M KCl, 2 mM $MgCl_2$, 1 mM DTT, 20 mM Hepes-NaOH, pH 7.5. Ultracentrifugation was performed with a Beckman Airfuge at 28 psi for 20 min. Control experiments were performed by replacing actin with 0.4 mg/ml BSA and nonspecific sedimentations of wild-type and mutant UNC-60B proteins were determined and subtracted from the data of the assays with actin. For the actin polymerization assays, *C. elegans* G-actin at 5 μM was incubated with UNC-60B proteins for 2 min in a buffer containing 2 mM Tris-HCl, 0.2 mM $CaCl_2$, 0.2 mM ATP, 0.2 mM DTT, pH 8.0, and polymerization was initiated at time 0 by adding salts at final concentrations of 0.1 M KCl, 2 mM $MgCl_2$, 0.2 mM EGTA, 20 mM Hepes-NaOH, pH 7.5. The kinetics of actin polymerization were monitored as changes in turbidity at a wavelength of 310 nm (Carlier et al., 1997) at 20°C. To determine the effects of UNC-60B proteins on the extent of actin polymerization, *C. elegans* G-actin at 5 μM was polymerized in the presence of UNC-60B proteins in a buffer containing 0.1 M KCl, 2 mM $MgCl_2$, 0.2 mM EGTA, 0.2 mM ATP, 0.2 mM DTT, 20 mM Hepes-NaOH, pH 7.5, for 4 h and the concentrations of the remaining G-actin were quantified with a DNase I inhibition assay as described (Blikstad et al., 1978; Heacock and Bamburg, 1983). It was established previously (Ono, 1999) that a DNase I inhibition assay is a valid measurement of *C. elegans* G-actin concentration.

Assay for Nucleation of Actin Polymerization

To determine whether wild-type and mutant UNC-60B proteins sever actin filaments and increase the filament ends, effects of UNC-60B proteins on the activity of F-actin to nucleate actin polymerization were examined as described (Hawkins et al., 1993; Hayden et al., 1993; Maciver et al., 1998). *C. elegans* F-actin at 10 μM was mixed for 30 s with 0–10 μM of wild-type or mutant UNC-60B in a buffer containing 0.1 M KCl, 2 mM $MgCl_2$, 0.1 mM ATP, 1 mM DTT, 20 mM Hepes-NaOH, pH 7.5. These

mixtures were added as nuclei at 1.25 μM actin to 2.5 μM pyrene-labeled G-actin and the changes in fluorescence of excitation at 366 nm and emission at 384 nm were monitored over time. The rates of nucleation for actin polymerization were determined as the initial rates of the increase in fluorescence intensity. The nucleation rates in the presence of UNC-60B proteins were divided by the rate of F-actin alone and expressed as the relative nucleation rates in Fig. 5. Pyrene-actin was prepared by labeling rabbit muscle actin with *N*-(1-pyrene) iodoacetamide (Molecular Probes Inc.) by the method of Kouyama and Mihashi (1981) and finally purified by gel filtration with Sephacryl S-300. The labeled G-actin was mixed with nonlabeled G-actin to make 10% pyrene-labeled G-actin and converted to MgATP–actin by incubating 5 μM of G-actin with 15 μM $MgCl_2$ and 0.2 mM EGTA for 3 min before the assay.

Production of Antibodies

Synthetic peptides that correspond to 15 amino acids from the COOH terminus of UNC-60A and UNC-60B and cysteine at the NH_2 terminus were synthesized and coupled to keyhole limpet hemocyanin by the Microchemical Facility at Emory University. The rabbit antisera against these conjugates were raised at Spring Valley Laboratories, Inc., and affinity-purified with Sepharose-6B columns to which the synthetic peptides had been immobilized.

Western Blot

Total SDS-soluble protein extracts from each strain (mostly adults) were prepared as described in Benian et al. (1996). Protein concentrations were determined by a filter paper dye-binding assay (Minamide and Bamburg, 1990). 10 μg of each lysate was separated on a 15% SDS–polyacrylamide gel and transferred onto polyvinylidene difluoride membrane (Immobilon-P; Millipore Corp.). The membranes were blocked in 5% nonfat milk in PBS containing 0.1% Tween 20 and incubated for 1 h with anti–UNC-60A, anti–UNC-60B, or antiactin (clone C4; ICN Pharmaceuticals, Inc.) antibodies followed by treatment with peroxidase-labeled donkey anti–rabbit or mouse IgG (Amersham Life Science). The reactivities were detected with a chemiluminescence reagent (Renaissance; NEN).

Immunofluorescence Microscopy

Immunofluorescent staining of whole adult nematodes was performed essentially as described (Benian et al., 1996). Immunofluorescent staining of embryos was performed by two methods. For double staining of myosin and UNC-60B, embryos were obtained by cutting gravid adults on polylysine-coated slides, freeze-cracked as described (Albertson, 1984; Epstein et al., 1993), fixed with −20°C methanol for 5 min, washed with PBS, and incubated with antibodies. The staining of actin was performed using the method of Barstead and Waterston (1991) with slight modifications. In brief, embryos were collected by a hypochlorite treatment of gravid adults, fixed with 4% paraformaldehyde in PBS for 10 min, permeabilized with −20°C methanol for 5 min, washed with PBS and 0.5% Triton X-100, and incubated with antibodies. In addition to anti–UNC-60B, we used antimyosin A mAb (clone 5.6) (Miller et al., 1983) and antiactin mAb (clone C4; ICN Pharmaceuticals, Inc.).

Results

Identification of UNC-60B as the Responsible Isoform for the Unc-60 Phenotype

To understand the function of a particular gene, availability of several different alleles allows us to correlate the properties of the gene products and the phenotypes. Viable *unc-60* alleles were previously described (Waterston et al., 1980; McKim et al., 1988) and the homozygous mutant animals show a wide range of phenotypic severity based on mobility (Fig. 1 A, Table I). Based upon our quantitative motility assay, they are from strongest to weakest alleles: *e677*, *m35*, *s1309*, *r398*, and *s1307*. All of them are recessive and hypomorphic because they exhibit more severe phenotypes when placed over a deficiency

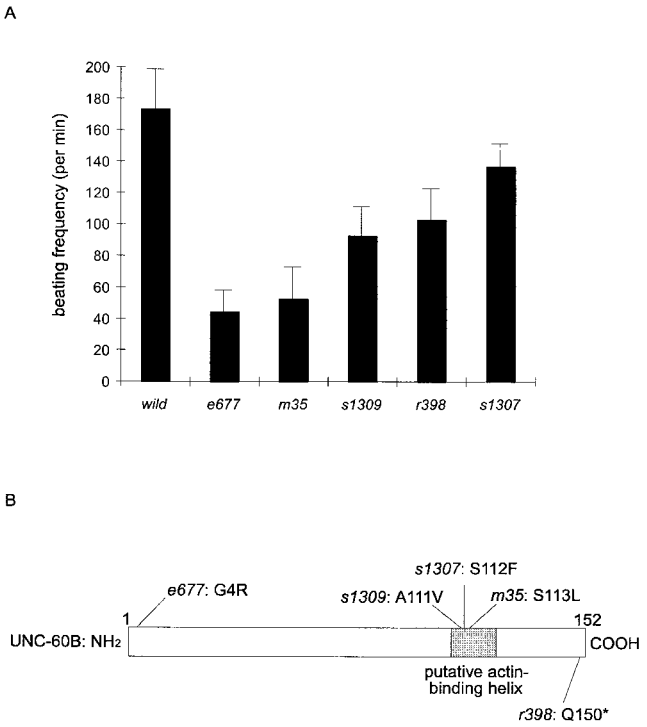

Figure 1. Motility of *unc-60* mutants and identification of mutation sites. (A) Motility of the adult *unc-60* mutant animals were scored by their beating frequencies in liquid. Values are the means ± SD, $n = 10$. (B) Sequence alterations in the *unc-60* mutants. The mutations are designated as the original residue, the position, the converted residue. The asterisk designates a stop codon. The gray region shows a putative actin-binding α-helix that was predicted from the homology between UNC-60B and yeast cofilin for which a structure has been solved.

(McKim et al., 1988), suggesting that the mutations cause partial defects in the function of the *unc-60* gene product.

Sequence analyses of the genomic DNA from the *unc-60* mutants showed that mutations in the unc-60B but not in the unc-60A coding region cause the Unc-60 phenotypes (Fig. 1 B). *s1309*, *m35*, and *s1307* have missense mutations within a region homologous in sequence to the α-helix that contains the putative actin-binding surface of the members of the ADF/cofilin family for which structures have been solved (Yonezawa et al., 1991; Hatanka et al, 1996; Fedorov et al., 1997; Leonard et al., 1997; Van Troys et al., 1997). *e723*, *s1310*, and *s1331* have the same mutation as *m35*. The missense mutation in *e677* lies close to the NH_2 terminus. *r398* has a premature stop codon that truncates three amino acids from the COOH terminus. Both the NH_2 terminus and the COOH terminus of ADF/cofilin have been implicated in binding to actin (Lappalainen et al., 1997). Thus, these sequence alterations suggest that the actin-binding activity of UNC-60B is changed in the *unc-60* mutants, but these alterations do not allow us to correlate the properties of the mutant proteins with the phenotypes. Therefore, we produced recombinant mutant UNC-60B proteins and examined their activities in vitro.

Effects of Mutant UNC-60B Proteins on F-actin

Mutant UNC-60B proteins showed various alterations in

Table I. Summary of the Phenotypes of unc-60 Mutants and the Properties of Mutant UNC-60B Proteins

	Alleles					
	Wild-type	*e677*	*m35*	*s1309*	*r398*	*s1307*
Motility[‡]	173 ± 28	44 ± 15	52 ± 21	92 ± 19	102 ± 26	136 ± 11
Mutations[§]	−	G4R	S113L	A111V	Q150*	S112F
Protein levels[‖]	1	<0.1	1.2	4.2	2.9	1.7
F-actin binding	++++	+++	++	++	+	+
Effects on depolymerization of F-actin	Partial	Partial	Very weak	Partial	Strong	Strong
Effects on actin polymerization	Accelerating	Weakly accelerating	Little effect	Little effect	Inhibiting	Accelerating (slightly inhibiting at actin/UNC-60B = 1:0.2)
Increase in unassembled actin	++	+	−	−	+	+++ (− at actin/UNC-60B = 1:0.2)
F-actin severing	+	−	−	−	−	+++

[‡]The data expressed in Fig. 1 A.
[§]Designated as the original residue/the position/the converted residue; *, stop codon.
[‖]The quantitative data of the Western blot in Fig. 6 B. The data represent the relative intensities of the signals to that of wild type (= 1).

their effects on F-actin as compared with wild type. Wild-type UNC-60B partially depolymerizes and also binds to *C. elegans* F-actin (Ono, 1999; Fig. 2 A). The extent of depolymerization of F-actin was consistent regardless of the concentration of UNC-60B and binding of UNC-60B to F-actin was saturated at a 1:1 molar ratio. *e677*, *m35*, and *s1309* showed weaker activities in both partial depolymerization and F-actin binding than wild type (Fig. 2, B–D). Maximum depolymerization was achieved by 5 μM of wild type (Fig. 2 A), but *e677* and *s1309* required 10 and 20 μM to reach the same level of depolymerization (Fig. 2, B and D). *m35* did not cause the equivalent level of depolymerization even at an extremely high concentration (80 μM, Fig. 2 C). These weak actin-depolymerization phenotypes probably indicate weak affinities of these mutants with ADP–G-actin. Weak binding of these mutants to F-actin was obvious because the amounts of these mutants that cosedimented with F-actin were lower than wild type at any equivalent concentrations examined here. Binding of *m35* and *s1309* to F-actin was so weak that saturation was not reached until 50 to 80 μM (Fig. 2, C and D).

Both *r398* and *s1307* showed stronger actin-depolymerizing and weaker F-actin binding than wild type (Fig. 2, E and F). When the concentrations of these mutants were increased, more F-actin was depolymerized (Fig. 2, E and F). In contrast, these mutants were poorly cosedimented with F-actin. However, a marked difference between these mutants was detected in the extent of depolymerization when their concentrations were substoichiometric to actin. At 5 μM of the mutants to 10 μM of F-actin, *s1307* showed greater actin-depolymerizing activity than *r398* (Fig. 2, E and F).

Effects of Mutant UNC-60B Proteins on Actin Polymerization

Wild-type UNC-60B strongly accelerated the rate of spontaneous polymerization of *C. elegans* actin (Fig. 3 A). However, all the mutant proteins were less potent in this effect than wild type to different extents (Fig. 3, B–F). In the presence of wild-type UNC-60B, the elongation phase of actin polymerization (200–1,000 s) was accelerated and the kinetics reached a plateau much earlier than actin alone (Fig. 3 A). This effect was obvious when UNC-60B was present at a concentration as low as 20% of actin in a molar ratio. The increases in turbidity in the later phase (after 1,000 s) were caused by binding of UNC-60B to F-actin that resulted in an increase in the mass of actin filaments (Carlier et al., 1997 and we confirmed by a pelleting assay). In contrast, *m35* and *s1309* showed only minor effects on the kinetics when these mutants were present at 1:1 molar ratio to actin (Fig. 3, C and D). Interestingly, *r398* had an inhibitory effect on the polymerization kinetics (Fig. 3 E). Although *e677* and *s1307* accelerated polymerization kinetics, both of them did not cause strong effects when they were present at 20% of actin, at which wild type can accelerate polymerization (Fig. 3, B and F, compare with A). In addition, acceleration by *e677* was less steep than wild type at the equivalent concentrations (Fig. 3 B). Acceleration by *s1307* was comparable to the effect of wild type, whereas the timing when the acceleration began was later for *s1307* (500–600 s) than for wild type (200 s) (Fig. 3 F).

Effects of wild-type and mutant UNC-60B proteins on the concentration of unassembled actin at steady state were determined quantitatively by a DNase I inhibition assay. In the presence of wild-type UNC-60B, the concentration of G-actin was increased (Fig. 4, closed circles). However, all the mutant proteins at 1 μM did not increase the concentration of G-actin in 5 μM of total actin (Fig. 4). *m35* and *s1309* did not affect the level of G-actin at any concentrations examined in this study. *e677* and *r398* increased the G-actin level to lesser extents than wild type only when they were present at 1:1 molar ratio to actin (Fig. 4, open circles and closed squares). Therefore, *m35*, *s1309*, *e677*, and *r398* are less active than wild type in this regard. However, *s1307* increased the G-actin concentration greater than wild type when *s1307* was present at >50% of actin (Fig. 4, open squares). Therefore, *s1307* is less active than wild type at low concentrations, but at high concentrations it shows hyperactivity in increasing the level of unpolymerized actin.

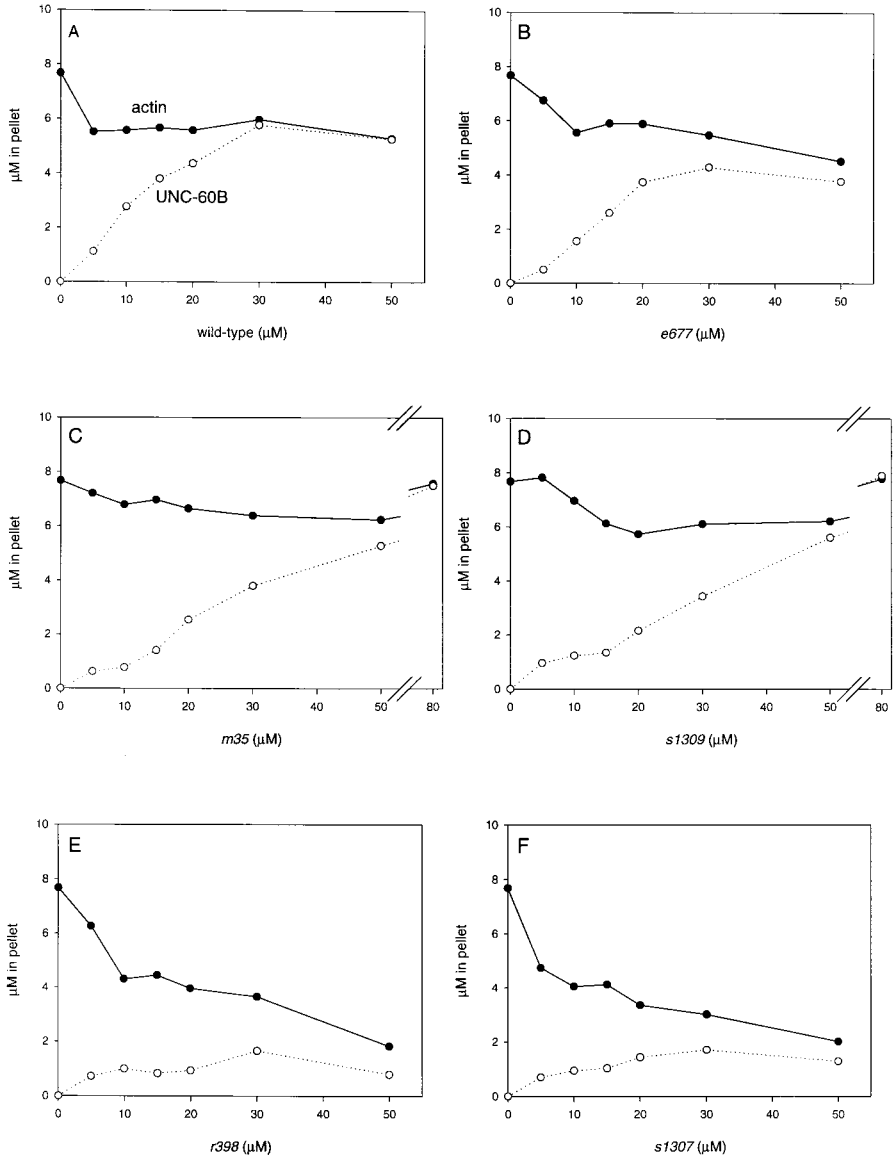

Figure 2. Effects of the mutant UNC-60B proteins on F-actin. *C. elegans* F-actin (10 μM) was incubated with various concentrations of wild-type or mutant UNC-60B proteins (horizontal axes; note that the scaling of C and D is different from the others) and the mixtures were examined by copelleting assays. On the vertical axes are plotted the sedimented portions (expressed as concentrations assuming that the pellets were reconstituted in the original volumes) of actin (closed circles with solid lines) and wild-type or mutant UNC-60B (open circles with dashed lines). Nonspecific sedimentations of wild-type or mutant UNC-60B were determined by control experiments as described in Materials and Methods and subtracted from the data of assays with actin. Data represent the average of two separate experiments.

Severing Activities of Mutant UNC-60B Proteins

Acceleration of actin polymerization by ADF/cofilin has been interpreted as its severing activity that increases filament ends (Du and Frieden, 1998; Maciver et al., 1991, 1998). Therefore, we tested whether wild-type and mutant UNC-60B sever actin filaments. As shown in Fig. 5 inset (closed circles), the elongation rate of actin polymerization from F-actin nuclei was increased by preincubating the nuclei with wild-type UNC-60B. This effect can be explained by fragmentation of the F-actin nuclei by UNC-60B that increased the number of filament ends (Maciver et al., 1998). The rate was increased by 30% at a 1:1 molar ratio of UNC-60B to actin subunits, suggesting that UNC-60B weakly severs actin filaments. In contrast, the *s1307* mutant remarkably increased the elongation rate to a much greater extent than wild type (Fig. 5, open squares). There was a threefold increase in the elongation rate at a 1:1 molar ratio of *s1307* to actin subunits, indicating that this mutant has much stronger actin-severing activity than wild type.

The other mutants, *e677*, *m35*, *s1309*, and *r398* did not increase the elongation rates (Fig. 5). It should be noted that *r398* decreased the elongation rate (Fig. 5 inset), suggesting that some actin filaments were depolymerized without being severed. These data provide supportive evidence for the turbidity measurements in Fig. 3 that wild type and *s1307* enhanced actin polymerization by severing actin filaments, whereas *e677*, *m35*, and *s1309* increased the turbidity by decorating actin filaments. However, a four- to fivefold increase in the polymerization rate in the presence of wild-type UNC-60B (Fig. 3 A) cannot be fully explained by a weak severing activity (a maximum of 30% increase in filament ends). Therefore, wild-type UNC-60B may also enhance association of actin monomers to barbed ends of actin filaments as reported for *Arabidopsis* ADF1 (Carlier et al., 1997). Our observations and interpretations are inconsistent with the report by Du and Frieden (1998) that fragmentation of actin filaments by yeast cofilin is sufficient to explain the enhanced rate of actin polymerization with the assumption that cofilin

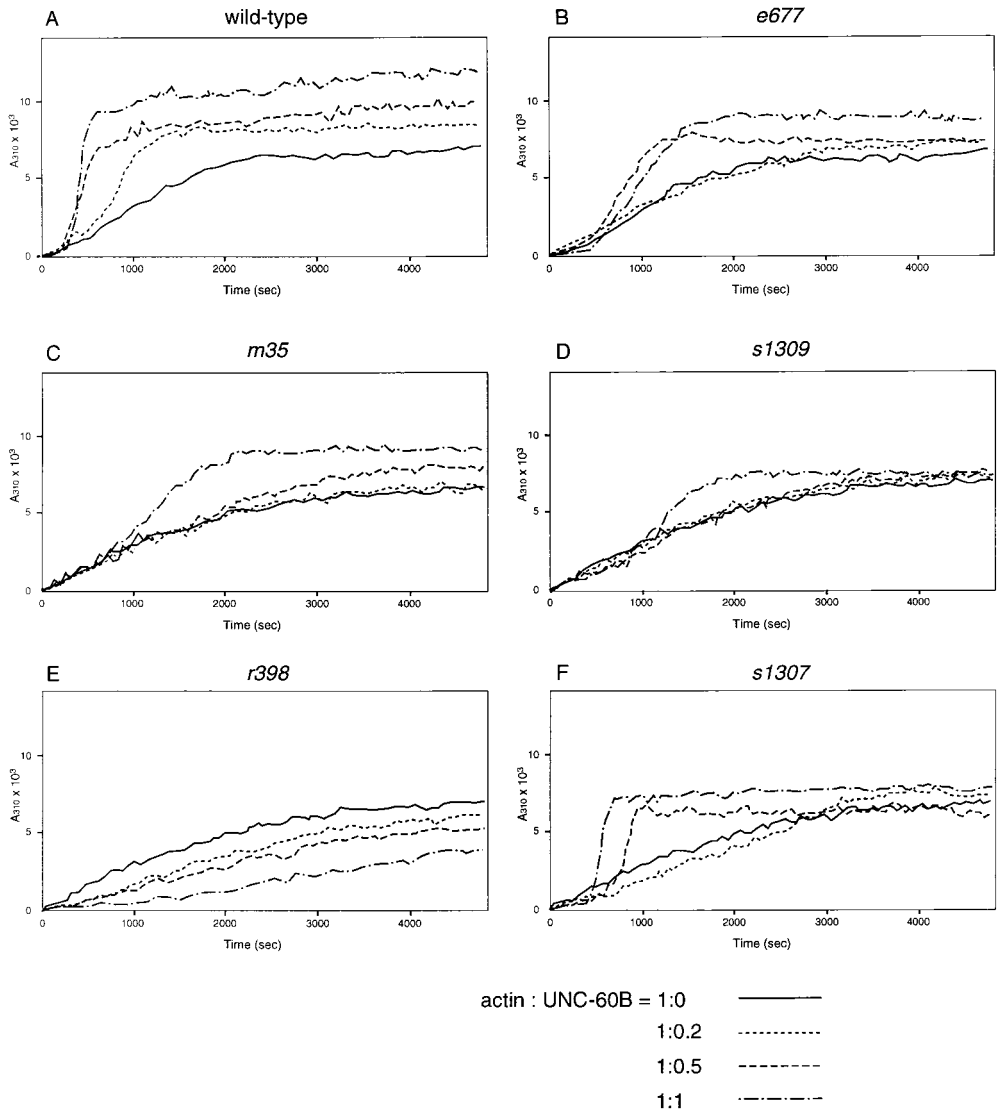

Figure 3. Effects of the mutant UNC-60B proteins on actin polymerization. *C. elegans* G-actin (5 μM) was incubated with the indicated molar ratios of wild-type or mutant UNC-60B, polymerization was started by adding salt (time 0), and the rates of polymerization were measured as changes in turbidity (absorbance at 310 nm) over time.

tightly binds ATP-G-actin and prevents polymerization. This inconsistency needs to be clarified by considering differences in experimental conditions, methods of analysis, and possible variances in the biochemical properties of ADF/cofilin isoforms.

Mutations in unc-60 Affect the Protein Levels of UNC-60B

As tools to identify UNC-60 proteins, we produced specific antibodies against UNC-60A and B using synthetic peptides as antigens (Fig. 6 A). Western blot analyses using these antibodies showed that the levels of UNC-60A were consistent among the homozygous mutant animals, whereas those of UNC-60B were variable (Fig. 6 B, Table I). The mutants, *m35* and *s1307*, contained moderately increased levels of UNC-60B as compared with wild type (Fig. 6 B, lanes 3 and 5). However, *r398* and *s1309* contained three- and fourfold larger amounts of UNC-60B as compared with wild type (Fig. 6 B, lanes 4 and 6). In contrast, *e677* had <10% (the lower limit of quantification of this Western blot) of UNC-60B as wild type (Fig. 6 B, lane 2). Although the band of UNC-60B in *e677* is not visible in Fig. 6 B, it appeared after a longer exposure of the blot.

UNC-60B Is Expressed in Embryonic Body Wall Muscle

UNC-60B was expressed in embryonic body wall muscle cells, supporting its function as an essential regulator of myofibril assembly during development. Although weak maternal expression of UNC-60B was observed (data not shown), its expression was remarkably upregulated in developing body wall muscle cells from the 1.5-fold stage (Fig. 7, a and b), when nascent myosin filaments were formed before obvious striations of myofibrils were established (Epstein et al., 1993). As myofibrils are assembled beneath the hypodermis in two- to threefold stages (Fig. 7 d), UNC-60B was localized both in diffuse cytoplasm and striated myofibrils (Fig. 7 c). The spindle-shaped outline of the muscle cells were visible by the UNC-60B staining, but the nuclei were devoid of staining (Fig. 7 c). In contrast,

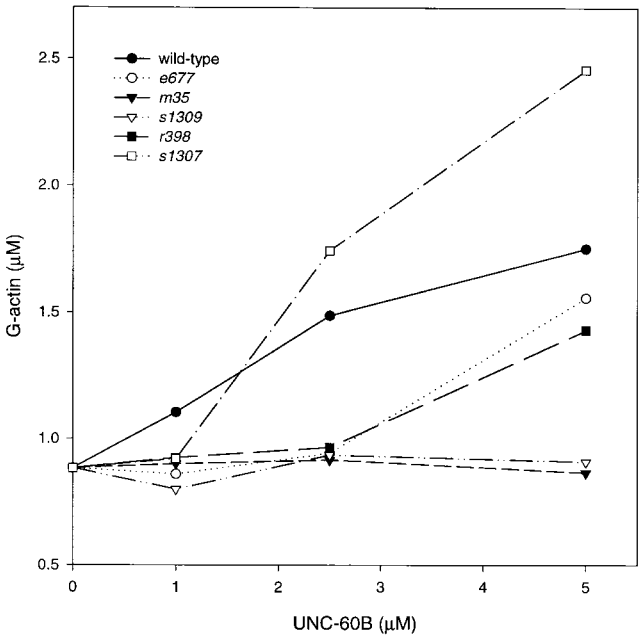

Figure 4. Effects of the mutant proteins on the concentration of unassembled actin. *C. elegans* actin at 5 μM was polymerized in the presence of wild-type or mutant UNC-60B for 4 h and the concentration of unpolymerized actin was quantified with a DNase I inhibition assay. Data represent averages of three experiments. Error bars are not included in the figure because they make the graph difficult to read. SDs of these data are <0.17 μM.

myosin staining was limited to the myofibrils. Because of the bright UNC-60B staining of diffuse cytoplasm, localization of UNC-60B in myofibrils was visible only in some areas of the image (Fig. 7 c, arrow). These data indicate that most of UNC-60B is diffusely located in the cytoplasm of embryonic muscle cells, suggesting that UNC-60B functions as a soluble regulator of actin polymerization in the cytoplasm of developing muscle cells.

In wild-type threefold stage embryos, actin was localized in myofibrils and the striation patterns were evenly distributed throughout the arrays of body wall muscle cells (Fig. 8 a). The staining of UNC-60B was found in body wall muscle cells in the same embryos, but it was diffuse and wider than the staining of actin, suggesting that UNC-60B was diffusely localized in cytoplasm, whereas actin is mostly assembled into myofibrils. We have noticed that the formaldehyde-methanol fixation optimized for actin staining gives less sharp staining of UNC-60B than the freeze-crack–methanol fixation (shown in Fig. 7). Especially, striated staining of UNC-60B and outlines of nuclei that were often clear by the freeze-crack–methanol fixation (Fig. 7 c) were not preserved in the formaldehyde–methanol-fixed embryos (Fig. 8 b).

Disorganization of myofibrils was observed in embryonic muscle cells of the *unc-60* mutants (Fig. 8). In the *unc-60* mutant embryos of the threefold stage, actin was found in discrete thick bundles that were not in the normal positions of thin filaments (Fig. 8, c, e, and g). Although *e677* shows a much more severe phenotype as adult worms than

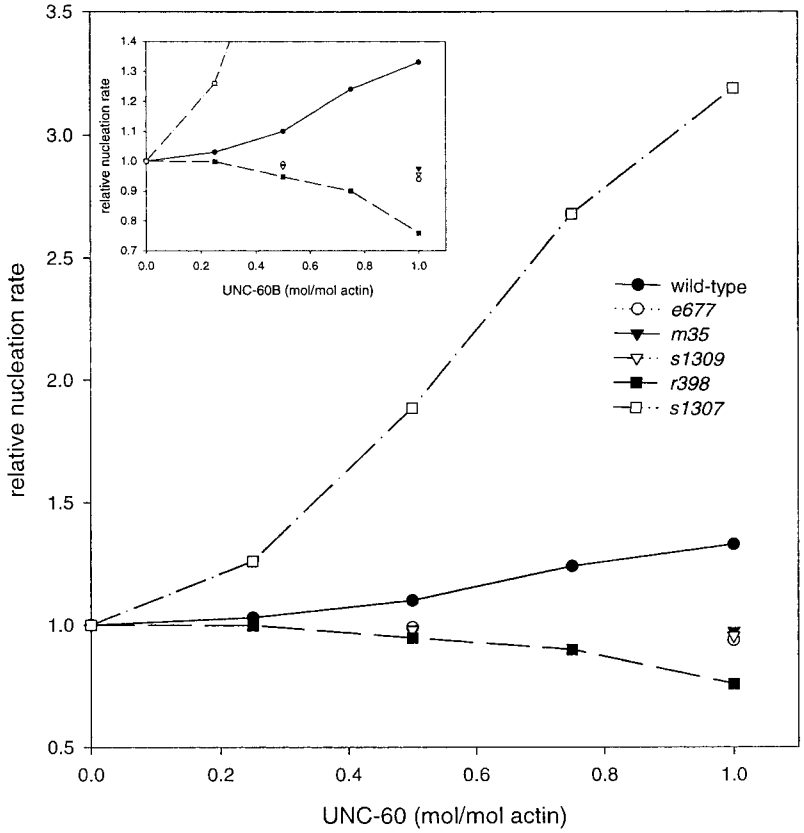

Figure 5. Effects of mutant UNC-60B on the nucleating activity of F-actin. *C. elegans* F-actin was mixed with wild-type or mutant UNC-60B and used as nuclei to induce polymerization of pyrene-labeled G-actin. The fluorescence of pyrene was measured over time and the initial rate of the increase in the fluorescence was taken as a nucleation rate. The inset is the same data with different scaling. The data are expressed as relative nucleation rates to that of F-actin alone. Data represent the average of two separate experiments.

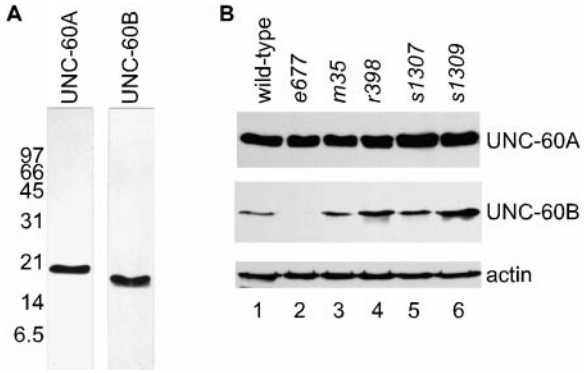

Figure 6. Changes in UNC-60B protein levels in *unc-60* mutants. (A) Specificity of anti–UNC-60A and anti–UNC-60B antibodies. Total lysates of wild-type nematodes were separated by SDS-PAGE, transferred onto a membrane and reacted with anti–UNC-60A or anti–UNC-60B antibodies. Each antibody specifically reacted with a single band of expected size, which was further confirmed by reactivity with either recombinant UNC-60A or UNC-60B (data not shown). Molecular mass markers in kD are indicated on the left. (B) Levels of UNC-60A and UNC-60B proteins in the *unc-60* mutant alleles. Only the level of UNC-60B protein varied among the alleles. The intensities of the bands of UNC-60B were quantified and shown in Table I. No alteration in the level of actin was observed.

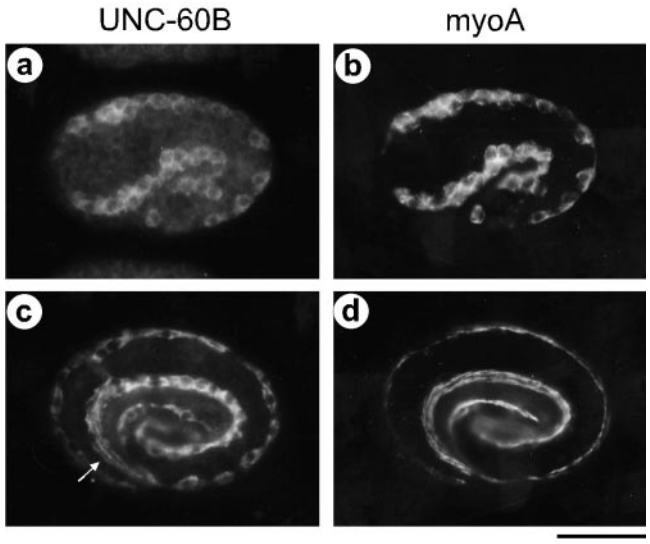

Figure 7. Expression of UNC-60B in embryonic body wall muscle. (a–d) Specific expression of UNC-60B in embryonic body wall muscle cells. 1.5-fold (a and b) and threefold (c and d) stage embryos were double-stained for UNC-60B (a and c) and body wall muscle–specific myosin heavy chain A (myoA) (b and d). An arrow in (c) indicates a region where UNC-60B is located in a striated pattern. Bar, 10 μm.

r398 (Fig. 1 A), they exhibited similar degrees of disorganization of actin in embryonic stages. The weakest mutant, *s1307*, also showed a high degree of disorganization of myofibrils in embryos (Fig. 8 g). The aggregates of actin in *s1307* were slightly larger than *e677* and *r398*, whereas the distribution of actin was discontinuous and was not found as organized myofibrils. In *e677*, only a trace level of UNC-60B protein was detected by the antibody staining (Fig. 8 d), which is consistent with the result of Western blot (Fig. 6 B). However, in *r398* and *s1307*, the immunostaining of UNC-60B was indistinguishable from that of wild type although the staining was not quantitative. These results suggest that the proper function of UNC-60B is critical for the process of actin filament assembly into myofibrils during embryonic stages.

unc-60 Mutants Show Aggregates of Actin and Disorganized Thick Filaments in Adult Body Wall Muscle

In adult animals carrying *unc-60* mutations, myofibrils of body wall muscle were highly disorganized, but exhibited a variety of disorganization depending upon the mutant alleles. In wild-type animals, myosin and actin were organized into striated sarcomeres (Fig. 9, a and b). Some UNC-60B was localized in a striated pattern (Fig. 9 c) and colocalized with actin by confocal microscopy (data not shown, see Discussion for details). In contrast, in *unc-60* mutant animals, large aggregates of actin were found at the ends of body wall muscle cells and myosin was also disorganized (Fig. 9, d–r). In the most severe mutant, *e677*, most of the actin was associated with the aggregates (Fig. 9 e) and myosin failed to form clear striations (Fig. 9 d). The staining of UNC–60B was only found in small dots in the muscle cells (Fig. 9 f), which was consistent with the low level of UNC-60B protein as shown by the Western blot (Fig. 6 B). In the second most severe mutant, *m35*, myosin was relatively aligned in striations (Fig. 9 g), although it was not as tight as in wild type (Fig. 9 a). However, most actin in *m35* was included in the large aggregates with UNC-60B and the occurrence of actin in striations was rare (Fig. 9 h). In the intermediate mutants, *s1309* and *r398*, actin was found in the aggregates with UNC-60B, whereas some actin formed a striated pattern (Fig. 9, k and l for *s1309*, n and o for *r398*). Myosin (Fig. 9, j and m) was disorganized to similar extents as *m35* (Fig. 9 g). The weakest mutant, *s1307*, showed relatively clear striations of myosin (Fig. 9 p), although the width of the striations were often greater than in wild type. The striated pattern of actin was clearer than in any of the other mutants (Fig. 9 q). Aggregates of actin in *s1307* were smaller than in the other mutants (Fig. 9 q). However, the mutant UNC-60B was associated preferentially with the aggregates rather than the thin filaments (Fig. 9 r). Thus, there was correlation between the severities in the slowness of movement and the extents of disorganization of myofibrils (Fig. 1 A and Table I). However, it is likely that these various phenotypes in adult muscles were caused by effects in the growth and/or the maintenance of myofibrils, because these mutants showed similar phenotypes in embryonic stages.

Discussion

Here, we described an essential role of a particular isoform of ADF/cofilin for proper assembly of actin into myofibrils. This was concluded from three major findings: mutations in UNC-60B, one of the two ADF/cofilin isoforms encoded by the *unc-60* gene, were sufficient to cause

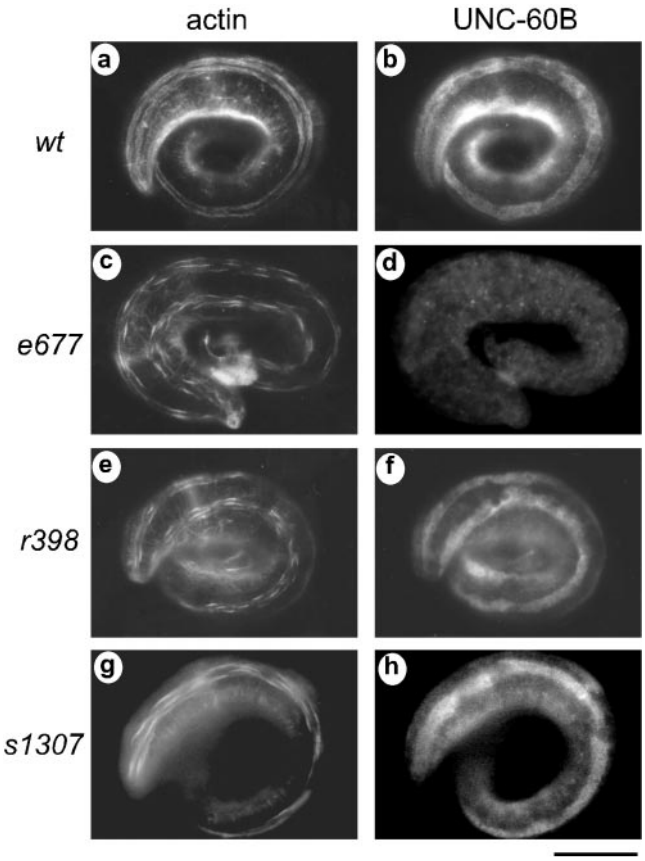

Figure 8. Disorganization of embryonic myofibrils in *unc-60* mutants. Immunofluorescent localization of actin (a, c, e, and g) and UNC-60B (b, d, f, and h) in threefold embryos of wild-type (a and b), *unc-60(e677)* (c and d), *unc-60(r398)* (e and f), and *unc-60(s1307)* (g and h) were observed by double staining and the same fields from each image are shown. Actin in wild-type (a) is continuous along the arrays of the body wall muscle cells. However, in the *unc-60* mutants (c, e and g), actin is found in discrete thick bundles. The extent of disorganization of myofibrils was indistinguishable between the most severe (c, *e677*) and second mildest (e, *r398*) mutants. The weakest mutant, *s1307* (g), showed somewhat larger bundles. Bar, 10 μm.

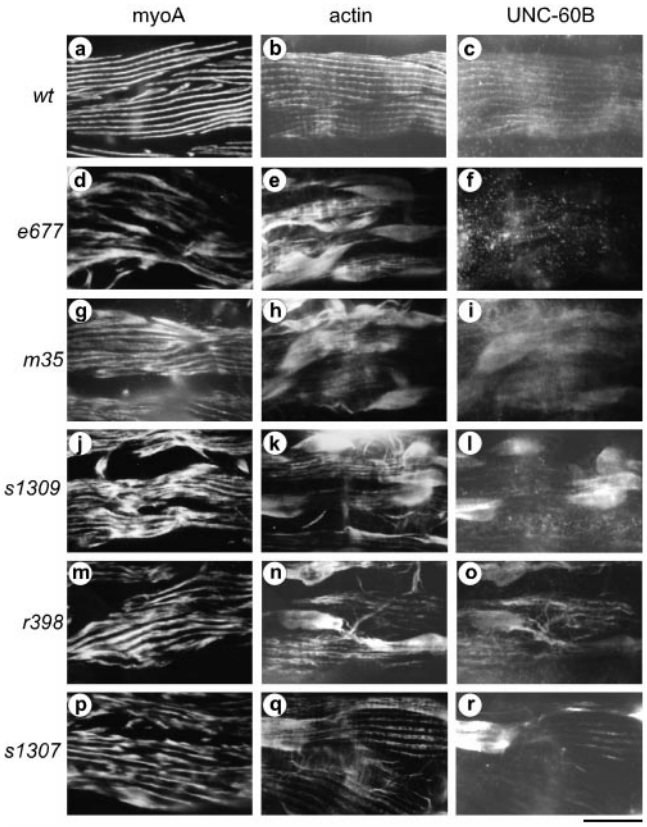

Figure 9. Disorganization of adult myofibrils in *unc-60* mutants. Localizations of myosin (myoA), actin, and UNC-60B in adult body wall muscle of the *unc-60* mutants were observed by immunofluorescence microscopy. Actin and UNC-60B were observed by double staining and the same fields from each image are shown. Bar, 10 μm.

disorganization of myofibrils; these mutations resulted in abnormal actin-regulating activities of UNC-60B; and UNC-60B was primarily expressed in body wall muscle cells during embryonic stages.

Function of UNC-60B as a Regulator of Actin Filament Dynamics

We detected three major in vitro functions for UNC-60B as an actin binding protein: F-actin binding activity, partial F-actin depolymerizing activity to maintain a high concentration of unassembled actin, and weak F-actin severing activity to accelerate actin polymerization. The combinations of biochemical and phenotypic consequences of each *unc-60* mutation as summarized in Table I suggests that UNC-60B is required to maintain a dynamic state of actin filaments. The most severe phenotype of *e677* is probably caused by its low level of UNC-60B protein rather than its reduced activity. The *m35* mutation also caused a severe phenotype, yet UNC-60B(*m35*) protein is present at an equivalent level to that of wild type. The severity of *m35* is due to its poor activity to enhance actin filament turnover. Although this mutant protein weakly binds to F-actin, it has no significant actin-depolymerizing activity (the weakest of the mutants) and no severing activity, which makes actin filaments poorly dynamic. This explanation also can be applied to *s1309*, whereas a weak actin-depolymerizing activity detected in a pelleting assay and a fourfold increase in the protein level probably improves its phenotype in the adult muscle as compared with *m35*. The phenotype of the *r398* mutant probably is caused by a lack of actin-severing activity in the mutant UNC-60B protein that failed to increase the number of barbed ends of actin where polymerization preferentially occurs. Nonetheless, its phenotype in adult muscle is not as severe as *e677* and *m35*, because the *r398* mutant protein has a stronger actin-depolymerizing activity than wild type probably by increasing the off rate of actin subunits from the pointed ends as previously demonstrated for other ADF/cofilins (Carlier et al., 1997; Maciver et al., 1998). However, this actin-depolymerizing activity is likely to be important in late development (larvae to adults), because the embryonic myofibrils of *r398* were highly disorganized and

nearly indistinguishable from those of *e677*, suggesting that the severing activity is important during the assembly of myofibrils. In contrast, the *s1307* mutation caused higher actin-depolymerizing and severing activities than wild type. Therefore, we can interpret that the phenotype of the *s1307* animals are caused by overenhancement of actin turnover, suggesting that the dynamics of actin filaments need to be maintained at a finely tuned level in order to assemble and maintain an organized actin cytoskeleton. This idea is supported by a report that microinjection of a high concentration of cofilin into nascent myotubes can disrupt myofibrils and induce formation of rodlike structures containing actin (Nagaoka et al., 1995).

However, it remains unclear why all the *unc-60* mutations cause similar phenotypes in embryonic muscle despite showing a variety of effects on the properties of UNC-60B protein. One possibility is that actin polymerization during myofibril assembly must be controlled tightly by UNC-60B, so that either hypoactive or hyperactive UNC-60B can easily disrupt the process of proper integration of actin into myofibrils. Even though the phenotypes of *unc-60* mutant embryos appeared similar by immunofluorescence microscopy, the other possibility is that the nature of the aggregates of actin in the mutants might be different. Studies on yeast cofilin mutants that are defective in the actin-depolymerizing activity have shown that these mutations cause slower actin filament turnover in actin patches (Lappalainen and Drubin, 1997; Lappalainen et al., 1997). Therefore, aggregated actin filaments in *e677*, *m35*, and *s1309* may be static, but those in *r398* and *s1307* may still be dynamic.

To understand the physiological relevance of our biochemical data, it would be informative to know the molar ratio of actin and UNC-60B in developing muscle cells. However, this is technically difficult to determine because methods to dissect embryonic worm muscle cells and/or culture systems for worm muscle are not available. The molar ratio of ADF/cofilin to actin varies from 0.17 to 0.64 in embryonic chicken tissues (Bamburg and Bray, 1987). In 10–d-old chicken embryonic muscles, the ratio of ADF/cofilin (the sum of ADF and cofilin) to actin is 0.14 (Nagaoka et al., 1996b). Assuming that embryonic muscles of the nematode maintain the similar ratio to chicken muscles, our data at an UNC-60B to actin ratio of 0.2:1 show that wild-type UNC-60B is able to accelerate actin polymerization (Fig. 3 A) and partially depolymerize F-actin (Fig. 4), but unable to significantly sever F-actin (Fig. 5). Nevertheless, we speculate that severing activity is an important function of UNC-60B because we observed that the *r398* mutation that abolished severing activity but not G-actin binding causes disorganization of myofibrils. This discrepancy is probably explained by the cooperative nature of binding between ADF/cofilin and F-actin (McGough et al., 1997). We preliminarily have observed that UNC-60B binds F-actin cooperatively by electron microscopy (McGough, A., and S. Ono, unpublished data). In addition, the sigmoidal curves of F-actin severing activity by wild-type and *s1307* mutant UNC-60B in Fig. 5 suggest that UNC-60B severs F-actin cooperatively. Therefore, it is possible that severing of a subset of actin filaments in muscle cells is important for actin filament dynamics in vivo.

Implications for the Interaction of ADF/Cofilins with Actin

Our studies on mutant UNC-60B provide important insights into the structural basis of the interaction of ADF/cofilins with actin. Four missense mutations that we identified occur at amino acid residues that are highly conserved among ADF/cofilin species (sequence alignments with other ADF/cofilins are shown by McKim et al., 1994), but none of these residues have been characterized by previous site-directed mutagenesis on ADF/cofilins (Moriyama et al., 1992; Agnew et al., 1995; Nagaoka et al., 1996a; Jiang et al., 1997; Lappalainen et al., 1997). Although a mutant maize ADF3, in which both Ala-104 (equivalent to Ala-111 of UNC-60B that is mutated in *s1309*) and Tyr-103 are altered, it has been shown to reduce its affinity to both G-actin and F-actin (Jiang et al., 1997), a role for this alanine on its own has not been characterized previously. However, we should consider that the mutations we identified here were selected for their effects on muscle function from a random mutagenesis and were not designed for a systematic mutagenesis, so that these mutations may alter or disrupt the structure of UNC-60B. It is quite informative that three mutations (*s1309*, *s1307*, and *m35*) occur within a putative actin binding helix that has been proposed by molecular modeling (Hatanaka et al., 1996; Wriggers et al., 1998) and a biochemical study using synthetic peptides (Yonezawa et al., 1991; Van Troys et al., 1997). Because these mutations changed small side chains (alanine or serine) to larger side chains (valine, phenylalanine, or leucine), they are likely to interfere with the interaction of the helix with actin, alter the integrity of the helix, or disrupt the intramolecular interaction of the helix with some other regions in UNC-60B. We are interested in the *s1307* mutation (S112F) that causes hyperactivity. Recent structural analysis by electron microscopy suggests that this mutant alters rabbit muscle actin filament by a greater extent than wild type (McGough et al., 1997; McGough, A., and S. Ono, unpublished data), which is a likely reason why this mutant causes stronger F-actin severing activity than wild-type. Currently, we are trying to understand this from molecular modeling of the structure of the mutant protein and reconstruction of the actin filaments that are decorated by the *s1307* mutant.

Our result that a small COOH-terminal truncation by the *r398* mutation impaired F-actin binding and severing activities provides evidence that the COOH terminus of ADF/cofilin is involved in F-actin binding. This is in agreement with the mutational analysis of yeast cofilin that has shown that mutations of charged amino acids in the COOH-terminal α–helix-4 abolished only F-actin binding but not G-actin binding (Lappalainen et al., 1997). However, the portion that is truncated in the *r398* mutant appeared to be closer to the COOH-terminal end than these mutations in yeast cofilin based on sequence alignments (McKim et al., 1994). Currently, it is difficult to predict how the COOH-terminal region is involved in F-actin binding, because this region is quite divergent among ADF/cofilin species and a high resolution structure of a complex of actin and ADF/cofilin has not been determined. Also, it is important that the *r398* mutation affects both F-actin binding and severing activities. This result

strongly supports the idea that two actin-binding sites are required to change the twist of F-actin resulting in the destabilization of actin filaments (McGough et al., 1997).

Expression and Localization of UNC-60B in Muscle Cells

UNC-60B was found to be expressed in embryonic body wall muscle cells before obvious myofibrils were formed, suggesting that UNC-60B is involved in the process of myofibril assembly. Localization of UNC-60B diffusely in the cytoplasm (Fig. 7, a and c) rather than in a structural component suggests its function as a regulator of actin filament dynamics in the cytoplasm. However, we noticed that intensity and location of the immunostaining of UNC-60B was variable depending on the methods of fixation. Among the methods that we tested, freeze-crack–methanol fixation that was used in Fig. 7 gave the brightest and sharpest staining of UNC-60B and appeared to reflect the real localization of UNC-60B. Permeabilization of worms by a detergent (0.1–0.5% Triton X-100) tended to lose UNC-60B and result in unclear diffuse staining of UNC-60B. For example, the staining patterns of UNC-60B in Fig. 8 showed slightly vague images, in which embryos were fixed with formaldehyde and permeabilized with methanol and 0.5% Triton X-100 to optimize the immunostaining of actin. Therefore, although we found localization of UNC-60B to adult myofibrils in Fig. 9, diffusely localized UNC-60B probably was lost in the course of extensive washing of fixed worms by 0.5% Triton X-100. Actually, when adult worms were fixed and permeabilized by a freeze-crack–methanol method, we observed a diffuse bright staining of UNC-60B in the cytoplasm, whereas the structures of myofibrils were not preserved well (data not shown). Our observation that UNC-60B is mainly localized in diffuse cytoplasm agrees with reports that ADF/cofilin is diffusely distributed in the cytoplasm of cultured chicken skeletal muscle cells (Abe et al., 1993; Ono et al., 1993).

Isoform-specific Function of ADF/Cofilins

Our finding that mutations in UNC-60B specifically cause defects in myofibril assembly provides the first evidence of an isoform-specific requirement of ADF/cofilin for assembly of a particular differentiated cytoskeletal structure. This is, in part, explained by the muscle-specific expression of UNC-60B. In contrast, UNC-60A was detected in almost all cells in embryos and a wide variety of cells in adult worms including body wall muscle (data not shown). However, more importantly, a functional difference between UNC-60A and UNC-60B probably contributes to the specific function of UNC-60B in muscle cells. We have reported previously that these two isoforms regulate actin filament dynamics in different manners (Ono and Benian, 1998), suggesting that UNC-60B can enhance actin filament dynamics to an optimal range for proper assembly of myofibrils. This speculation is supported by our results that either hypoactive or hyperactive mutant UNC-60B can cause defects in myofibril assembly,

Mammals have a muscle-specific isoform of cofilin (M-cofilin; Ono et al., 1994). M-cofilin is expressed in heart and skeletal muscle and upregulated upon differentiation of cultured myogenic cell lines (Ono et al., 1994). Although its intracellular localization and function are yet to be characterized, we expect that M-cofilin has functional similarity to UNC-60B. However, an alignment and a phylogenetic analysis of amino acid sequences of the ADF/cofilin family has shown that UNC-60B does not exhibit outstanding similarity to M-cofilin (Lappalainen et al., 1998). The sequence of UNC-60B is most related to UNC-60A and equally similar to three vertebrate ADF/cofilins (ADF, M-cofilin, and nonmuscle-type cofilin). Also, we could not detect any regions commonly unique to UNC-60B and M-cofilin. Therefore, M-cofilin probably has been evolved specifically for the structure and function of skeletal muscle in vertebrates. Nevertheless, because of the conservation of muscle components and architecture in all animals, we believe that there should be a protein, possibly M-cofilin, with a function similar to UNC-60B in mammalian cells.

The authors thank Dr. D. Miller for antimyosin antibody, Drs. J. Bamburg (Colorado State University, Fort Collins, Colorado), S. Maciver (University of Edinburgh), A. McGough (Baylor College of Medicine, Houston, Texas), and A. Weeds (MRC Laboratory of Molecular Biology) for helpful discussion and suggestions and Drs. W. Sale, H. Joshi, S. L'Hernault, K. Bhat, and T. Tinley (Emory University, Atlanta, Georgia) for critical reading of the manuscript.

This work was supported by a grant from the National Science Foundation (MCB-9728762) to S. Ono and G.M. Benian, a grant from the National Sciences and Engineering Research Council to D.L. Baillie, and a postdoctoral fellowship from the Uehara Memorial Foundation to S. Ono.

Received for publication 3 February 1999 and in revised form 18 March 1999.

References

Abe, H., and T. Obinata. 1989. An actin-depolymerizing protein in embryonic chicken skeletal muscle: purification and characterization. *J. Biochem.* 106: 172–180.

Abe, H., S. Ohshima, and T. Obinata. 1989. A cofilin-like protein is involved in the regulation of actin assembly in developing skeletal muscle. *J. Biochem.* 106:696–702.

Abe, H., R. Nagaoka, and T. Obinata. 1993. Cytoplasmic localization and nuclear transport of cofilin in cultured myotubes. *Exp. Cell Res.* 206:1–10.

Abe, H., T. Obinata, L.S. Minamide, and J.R. Bamburg. 1996. *Xenopus laevis* actin-depolymerizing factor/cofilin: a phosphorylation-regulated protein essential for development. *J. Cell Biol.* 132:871–885.

Agnew, B.J., L.S. Minamide, and J.R. Bamburg. 1995. Reactivation of phosphorylated actin depolymerizing factor and identification of the regulatory site. *J. Biol. Chem.* 270:17582–17587.

Aizawa, H., K. Sutoh, and I. Yahara. 1996. Overexpression of cofilin stimulates bundling of actin filaments, membrane ruffling, and cell movement in *Dictyostelium*. *J. Cell Biol.* 132:335–344.

Albertson, D.G. 1984. Formation of the first cleavage spindle in nematode embryos. *Dev. Biol.* 101:61–72.

Bamburg, J.R. and D. Bray. 1987. Distribution and cellular localization of actin depolymerizing factor. *J. Cell Biol.* 105:2817–2825.

Bamburg, J.R., H.E. Harris, and A.G. Weeds. 1980. Partial purification and characterization of an actin depolymerizing factor from brain. *FEBS (Fed. Eur. Biochem. Soc.) Lett.* 121:178–182.

Barstead, R.J., and R.H. Waterston. 1991. Vinculin is essential for muscle function in the nematode. *J. Cell Biol.* 114:715–724.

Benian, G.M., T.L. Tinley, X. Tang, and M. Borodovsky. 1996. The *Caenorhabditis elegans* gene *unc-89*, required for muscle M-line assembly, encodes a giant modular protein composed of Ig and signal transduction domains. *J. Cell Biol.* 132:835–848.

Blikstad, I., F. Markey, L. Carlsson, T. Persson, and U. Lindberg. 1978. Selective assay of monomeric and filamentous actin in cell extracts, using inhibition of deoxyribonuclease I. *Cell.* 15:935–943.

Carlier, M.F., V. Laurent, J. Santolini, R. Melki, D. Didry, G.X. Xia, Y. Hong, N.H. Chua, and D. Pantaloni. 1997. Actin depolymerizing factor (ADF/cofilin) enhances the rate of filament turnover: implication in actin-based motility. *J. Cell Biol.* 136:1307–1322.

Du, J., and C. Frieden. 1998. Kinetic studies on the effect of yeast cofilin on yeast actin polymerization. *Biochemistry.* 37:13276–13284.

Eddy, R.J., J. Han, and J.S. Condeelis. 1997. Capping protein terminates but does not initiate chemoattractant-induced actin assembly in *Dictyostelium*. *J. Cell Biol.* 139:1243–1253.

Epstein, H.F., and J.N. Thomson. 1974. Temperature-sensitive mutation affecting myofilament assembly in *Caenorhabditis elegans. Nature.* 250:579–580.

Epstein, H.F., D.L. Casey, and I. Ortiz. 1993. Myosin and paramyosin of *Caenorhabditis elegans* embryos assemble into nascent structures distinct from thick filaments and multifilament assemblages. *J. Cell Biol.* 122:845–858.

Fedorov, A.A., P. Lappalainen, E.V. Fedorov, D.G. Drubin, and S.C. Almo. 1997. Structure determination of yeast cofilin. *Nat. Struct. Biol.* 4:366–369.

Gill, S.C., and P.H. von Hippel. 1989. Calculation of protein extinction coefficients from amino acid sequence data. *Anal. Biochem.* 182:319–326.

Gregorio, C.C., A. Weber, M. Bondad, C.R. Pennise, and V.M. Fowler. 1995. Requirement of pointed-end capping by tropomodulin to maintain actin filament length in embryonic chick cardiac myocytes. *Nature.* 377:83–86.

Gunsalus, K.C., S. Bonaccorsi, E. Williams, F. Verni, M. Gatti, and M.L. Goldberg. 1995. Mutations in *twinstar*, a *Drosophila* gene encoding a cofilin/ADF homologue, result in defects in centrosome migration and cytokinesis. *J. Cell Biol.* 131:1243–1259.

Hatanaka, H., K. Ogura, K. Moriyama, S. Ichikawa, I. Yahara, and F. Inagaki. 1996. Tertiary structure of destrin and structural similarity between two actin-regulating protein families. *Cell.* 85:1047–1055.

Hawkins, M., B. Pope, S.K. Maciver, and A.G. Weeds. 1993. Human actin depolymerizing factor mediates a pH-sensitive destruction of actin filaments. *Biochemistry.* 32:9985–9993.

Hayakawa, K., N. Minami, S. Ono, Y. Ogasawara, T. Totsuka, H. Abe, T. Tanaka, and T. Obinata. 1993. Increased expression of cofilin in dystrophic chicken and mouse skeletal muscles. *J. Biochem.*114:582–587.

Hayden, S.M., P.S. Miller, A. Brauweiler, and J.R. Bamburg. 1993. Analysis of the interactions of actin depolymerizing factor with G- and F-actin. *Biochemistry*. 32:9994–10004.

Heacock, C.S., and J.R. Bamburg. 1983. The quantitation of G- and F-actin in cultured cells. *Anal. Biochem*. 135:22–36.

Jiang, C.J., A.G. Weeds, S. Khan, and P.J. Hussey. 1997. F-actin and G-actin binding are uncoupled by mutation of conserved tyrosine residues in maize actin depolymerizing factor (ZmADF). *Proc. Natl. Acad. Sci. USA*. 94:9973–9978.

Kouyama, T., and K. Mihashi. 1981. Fluorimetry study of *N*-(1-pyrenyl)iodoacetamide-labelled F-actin. Local structural change of actin protomer both on polymerization and on binding of heavy meromyosin. *Eur. J. Biochem*. 114:33–38.

Lappalainen, P., and D.G. Drubin. 1997. Cofilin promotes rapid actin filament turnover in vivo. *Nature.* 388:78–82.

Lappalainen, P., E.V. Fedorov, A.A. Fedorov, S.C. Almo, and D.G. Drubin. 1997. Essential functions and actin-binding surfaces of yeast cofilin revealed by systematic mutagenesis. *EMBO (Eur. Mol. Biol. Organ.) J.* 16:5520–5530.

Lappalainen, P., M.M. Kessels, M.J. Cope, and D.G. Drubin. 1998. The ADF homology (ADF-H) domain: a highly exploited actin-binding module. *Mol. Biol. Cell.* 9:1951–1959.

Leonard, S.A., A.G. Gittis, E.C. Petrella, T.D. Pollard, and E.E. Lattman. 1997. Crystal structure of the actin-binding protein actophorin from *Acanthamoeba*. *Nat. Struct. Biol.* 4:369–373.

Lopez, I., R.G. Anthony, S.K. Maciver, C.J. Jiang, S. Khan, A.G. Weeds, and P.J. Hussey. 1996. Pollen specific expression of maize genes encoding actin depolymerizing factor-like proteins. *Proc. Natl. Acad. Sci. USA*. 93:7415–7420.

Maciver, S.K., B.J. Pope, S. Whytock, and A.G. Weeds. 1998. The effect of two actin depolymerizing factors (ADF/cofilins) on actin filament turnover: pH sensitivity of F-actin binding by human ADF, but not of *Acanthamoeba* actophorin. *Eur. J. Biochem.* 256:388–397.

Maciver, S.K., H.G. Zot, and T.D. Pollard. 1991. Characterization of actin filament severing by actophorin from *Acanthamoeba castellanii*. *J. Cell Biol.* 115:1611–1620.

McGough, A., B. Pope, W. Chiu, and A. Weeds. 1997. Cofilin changes the twist of F-actin: implications for actin filament dynamics and cellular function. *J. Cell Biol.* 138:771–781.

McKim, K.S., C. Matheson, M.A. Marra, M.F. Wakarchuk, and D.L. Baillie. 1994. The *Caenorhabditis elegans unc-60* gene encodes proteins homologous to a family of actin-binding proteins. *Mol. Gen. Genet.* 242:346–357.

McKim, K.S., M.F. Heschl, R.E. Rosenbluth, and D.L. Baillie. 1988. Genetic organization of the *unc-60* region in *Caenorhabditis elegans*. *Genetics.* 118: 49–59.

Miller, D.M., I. Ortiz, G.C. Berliner, and H.F. Epstein. 1983. Differential localization of two myosins within nematode thick filaments. *Cell.* 34:477–490.

Minamide, L.S., and J.R. Bamburg. 1990. A filter paper dye-binding assay for quantitative determination of protein without interference from reducing agents or detergents. *Anal. Biochem.* 190:66–70.

Moon, A., and D.G. Drubin. 1995. The ADF/cofilin proteins: stimulus-responsive modulators of actin dynamics. *Mol. Biol. Cell.* 6:1423–1431.

Moriyama, K., E. Nishida, N. Yonezawa, H. Sakai, S. Matsumoto, K. Iida, and I. Yahara. 1990. Destrin, a mammalian actin-depolymerizing protein, is closely related to cofilin. Cloning and expression of porcine brain destrin cDNA. *J. Biol. Chem.* 265:5768–5773.

Moriyama, K., N. Yonezawa, H. Sakai, I. Yahara, and E. Nishida. 1992. Mutational analysis of an actin-binding site of cofilin and characterization of chimeric proteins between cofilin and destrin. *J. Biol. Chem.* 267:7240–7244.

Nagaoka, R., K. Kusano, H. Abe, and T. Obinata. 1995. Effects of cofilin on actin filamentous structures in cultured muscle cells. Intracellular regulation of cofilin action. *J. Cell Sci.* 108:581–593.

Nagaoka, R., H. Abe, and T. Obinata. 1996a. Site-directed mutagenesis of the phosphorylation site of cofilin: its role in cofilin-actin interaction and cytoplasmic localization. *Cell Motil. Cytoskeleton.* 35:200–209.

Nagaoka, R., N. Minami, K. Hayakawa, H. Abe, and T. Obinata. 1996b. Quantitative analysis of low molecular weight G-actin-binding proteins, cofilin, ADF and profilin, expressed in developing and degenerating chicken skeletal muscles. *J. Muscle Res. Cell Motil.* 17:463–473.

Nishida, E., S. Maekawa, and H. Sakai. 1984. Cofilin, a protein in porcine brain that binds to actin filaments and inhibits their interactions with myosin and tropomyosin. *Biochemistry.* 23:5307–5313.

Ohshima, S., H. Abe, and T. Obinata. 1989. Isolation of profilin from embryonic chicken skeletal muscle and evaluation of its interaction with different actin isoforms. *J. Biochem.* 105:855–857.

Ono, S. 1999. Purification and biochemical characterization of actin from *Caenorhabditis elegans*: its difference from rabbit muscle actin in the interaction with nematode ADF/cofilin. *Cell Motil. Cytoskeleton.* In press.

Ono, S., and G.M. Benian. 1998. Two *Caenorhabditis elegans* actin depolymerizing factor/cofilin proteins, encoded by the *unc-60* gene, differentially regulate actin filament dynamics. *J. Biol. Chem.* 273:3778–3783.

Ono, S., H. Abe, R. Nagaoka, and T. Obinata. 1993. Colocalization of ADF and cofilin in intranuclear actin rods of cultured muscle cells. *J. Muscle Res. Cell Motil.* 14:195–204.

Ono, S., N. Minami, H. Abe, and T. Obinata. 1994. Characterization of a novel cofilin isoform that is predominantly expressed in mammalian skeletal muscle. *J. Biol. Chem.* 269:15280–15286.

Rosenblatt, J., B.J. Agnew, H. Abe, J.R. Bamburg, and T.J. Mitchison. 1997. *Xenopus* actin depolymerizing factor/cofilin (XAC) is responsible for the turnover of actin filaments in *Listeria monocytogenes* tails. *J. Cell Biol.* 136: 1323–1332.

Schafer, D.A., C. Hug, and J.A. Cooper. 1995. Inhibition of CapZ during myofibrillogenesis alters assembly of actin filaments. *J. Cell Biol.* 128:61–70.

Shimizu, N., and T. Obinata. 1986. Actin concentration and monomer-polymer ratio in developing chicken skeletal muscle. *J. Biochem.* 99:751–759.

Van Troys, M., D. Dewitte, J.L. Verschelde, M. Goethals, J. Vandekerckhove, and C. Ampe. 1997. Analogous F-actin binding by cofilin and gelsolin segment 2 substantiates their structural relationship. *J. Biol. Chem.* 272:32750–32758.

Waterston, R.H., J.N. Thomson, and S. Brenner. 1980. Mutants with altered muscle structure of *Caenorhabditis elegans*. *Dev. Biol.* 77:271–302.

Wriggers, W., J.X. Tang, T. Azuma, P.W. Marks, and P.A. Janmey. 1998. Cofilin and gelsolin segment-1: molecular dynamics simulation and biochemical analysis predict a similar actin binding mode. *J. Mol. Biol.* 282:921–932.

Xu, J., J.F. Casella, and T.D. Pollard. 1999. Effect of capping protein, CapZ, on the length of actin filaments and mechanical properties of actin filament networks. *Cell Motil. Cytoskeleton.* 42:73–81.

Yonezawa, N., E. Nishida, K. Iida, H. Kumagai, I. Yahara, and H. Sakai. 1991. Inhibition of actin polymerization by a synthetic dodecapeptide patterned on the sequence around the actin-binding site of cofilin. *J. Biol. Chem.* 266: 10485–10489.